DE-Vol. 84-2, 1995 Design Engineering Technical Conferences
Volume 3 – Part B
ASME 1995

A MULTI-FIELD SPACE-TIME FINITE ELEMENT METHOD FOR STRUCTURAL ACOUSTICS

Lonny L. Thompson

Department of Mechanical Engineering
Clemson University
Clemson, South Carolina 29634-0921

ABSTRACT

A Computational Structural Acoustics (CSA) capability for solving scattering, radiation, and other problems related to the acoustics of submerged structures has been developed by employing some of the recent algorithmic trends in Computational Fluid Dynamics (CFD), namely time-discontinuous Galerkin Least-Squares finite element methods. Traditional computational methods toward simulation of acoustic radiation and scattering from submerged elastic bodies have been primarily based on frequency domain formulations. These classical time-harmonic approaches (including boundary element, finite element, and finite difference methods) have been successful for problems involving a limited range of frequencies (narrow band response) and scales (wavelengths) that are large compared to the characteristic dimensions of the elastic structure. Attempts at solving large-scale structural acoustic systems with dimensions that are much larger than the operating wavelengths and which are complex, consisting of many different components with different scales and broadband frequencies, has revealed limitations of many of the classical methods. As a result, there has been renewed interest in new innovative approaches, including time-domain approaches. This paper describes recent advances in the development of a new class of high-order accurate and unconditionally stable space-time methods for structural acoustics which employ finite element discretization of the time domain as well as the usual discretization of the spatial domain. The formulation is based on a space-time variational equation for both the acoustic fluid and elastic structure together with their interaction. Topics to be discussed include the development and implementation of higher-order accurate non-reflecting boundary conditions based on the exact impedance relation through the Dirichlet-to-Neumann (DtN) map, and a multi-field representation for the acoustic fluid based on independent pressure and velocity potential variables. Numerical examples involving radiation and scattering of acoustic waves are presented to illustrate the high-order accuracy achieved by the new methodology for CSA.

INTRODUCTION

Previous approaches to the transient structural acoustics problem involving the interaction of vibrating structures submerged in an infinite acoustic fluid have employed (i) boundary element methods based on Kirchhoff's retarded potential integral formulation [1, 2], (ii) Taylor-Galerkin methods, e.g. [3], and (iii) semi-discrete methods which employ standard Galerkin finite element methods in space and finite difference techniques for integrating in time (also referred to as the method of lines), see e.g. [4, 5, 6, 7]. However for general transient wave propagation problems it is well known that these standard methods are not optimal. This is especially evident for problems involving sharp gradients in the solution which typically arise in the vicinity of fluid-structure interfaces and near inhomogeneities such as stiffeners and structural joints. In this paper a new multi-field space-time finite element approach to solving the coupled structural acoustics problem is described. The proposed method employs the

simultaneous discretization of the spatial and temporal domains and is based on a new time-discontinuous variational formulation for the coupled fluid-structure system.

Discontinuous Galerkin (DG) space-time methods with residual based stabilization such as Galerkin Least-Squares (GLS) methods have been shown to be effective for first-order and second-order hyperbolic systems of partial differential equations, see e.g. [8, 9, 10, 11, 12], and are now widely used in many applications arising in computational fluid dynamics (CFD), including problems governed by the compressible Euler and Navier-Stokes equations [13, 14], advection-diffusion problems [15], and large-eddy and turbulence modeling [16]. In this approach, the concept of space-time slabs is employed which allow for discretizations that are discontinuous in time and offers great flexibility in the discretization; in particular through the possibility of using space-time meshes oriented along space-time characteristics.

Recently, the time-discontinuous space-time finite element method has been successfully extended to the second-order hyperbolic equations governing structural acoustics in infinite domains [17, 18, 19, 20, 21, 22]. In these single-field formulations, scalar velocity potential is used as the solution variable for the acoustic fluid, while the displacement vector is used to represent the motion of the structure. Since these methods use a single trial solution in each physical region, in this case the structural domain and surrounding fluid domain, they are referred to as 'single-field' formulations. In this paper, an extension of the single-field time-discontinuous space-time formulation for structural acoustics is presented where independent finite element approximations are used for the structural displacement vector and its time derivative, together with independent approximations for the acoustic pressure and velocity potential. For this multi-field formulation, the resulting system of coupled algebraic equations to be solved in each time step takes on a positive form; a condition which is necessary for the unconditional stability of the algorithm for unstructured space-time meshes.

The resulting multi-field space-time algorithm gives a general solution to the fundamental problem of constructing a finite element method for transient structural acoustics with the desired combination of good stability and high accuracy. Stability is obtained through the introduction of temporal jump operators which weakly enforce continuity of the independent solution variables between space-time slabs. Additional stability is obtained by a Galerkin Least-Squares (GLS) modification. The order of accuracy of the solution is related to the order of the finite element spatial and temporal basis functions chosen, and can be specified to any accuracy and for general unstructured discretizations in space and time.

In addition to the advantages cited above, the space-time finite element approach provides a powerful framework for unified and simultaneous spatial and temporal adaptivity of the discretization. This is especially useful in the application of self-adaptive solution strategies for transient structural acoustics, in which both spatial and temporal enhancement can efficiently capture waves propagating along space-time characteristics. Furthermore the use of space-time hp-adaptive discretization strategies, where a combination of mesh size refinement/unrefinement (h-adaptivity), and finite element basis enrichment (p-adaptivity), can easily be accommodated in the time-discontinuous formulation. Because the temporal and spatial domains are treated in a consistent manner in the space-time variational equations, the method gives rise to a firm mathematical foundation from which rigorous *a posteriori* error estimates useful for reliable and efficient adaptive schemes may be established, see e.g. [23].

For the approach presented here, a truncated fluid domain with radiation (non-reflecting) boundary conditions is employed to transmit outgoing waves to infinity. For large-scale, three-dimensional discretizations, the use of accurate radiation boundary conditions is essential to allow the fluid truncation boundary to be placed close to the structure, minimizing the mesh and matrix problem size. New, high-order accurate non-reflecting boundary conditions, based on the exact impedance relation through the Dirichlet-to-Neumann (DtN) map [24], will be described. Details for the implementation of the first two operators in the localized DtN non-reflecting boundary conditions in the new multi-field formulation are described; further details on the derivation and implementation in single-field formulations are given in [18, 17, 20].

THE STRUCTURAL ACOUSTICS PROBLEM

Consider the coupled system consisting of a structural region Ω_s in $\mathbb{R}^{n_{sd}}$; where n_{sd} is the number of space dimensions, surrounded by an infinite fluid region $\mathcal{B}$. The interface boundary between the structure and fluid domains is denoted by Γ_i. The unit outward normal to the structure (inward normal to the fluid) on Γ_i is denoted by $\boldsymbol{n}$.

The structure is assumed to be governed by the equations of elastodynamics while the fluid equations are taken under the usual linear acoustic assumptions of an inviscid, compressible fluid with small disturbance. The

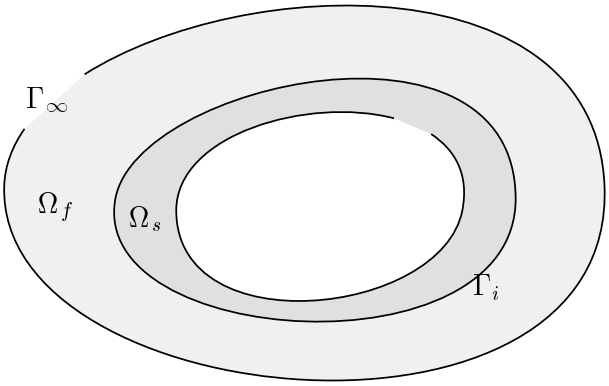

Fig. 1: Coupled system for the exterior fluid-structure interaction problem, with artificial boundary Γ_∞ enclosing the finite computational domain $\Omega = \Omega_f \cup \Omega_s$.

momentum equations for small motions of an acoustic fluid are

$$\nabla p + \rho_f \dot{\boldsymbol{v}} = \boldsymbol{0} \tag{1}$$

where $p(\boldsymbol{x}\,,\,t)$ is the excess pressure perturbation from the static pressure, $\boldsymbol{v}(\boldsymbol{x}\,,\,t)$ is the fluid particle velocity, and $\rho_f = \rho_f(\boldsymbol{x}) > 0$ is the density of the fluid. A superimposed dot indicates partial differentiation with respect to time t. The constitutive behavior of the fluid is assumed to be

$$\dot{p} + K_f \nabla \cdot \boldsymbol{v} = 0 \tag{2}$$

where $K_f = \rho_f c^2$ is the bulk modulus of the fluid and c is the acoustic wave speed. From the assumption of an irrotational acoustic fluid, the velocity can be written as the gradient of the velocity potential ϕ as $\boldsymbol{v} = \nabla\phi$. Consequently, pressure is related to the velocity potential by $p = -\rho_f \dot{\phi}$.

On the structural interface Γ_i, the normal component of the fluid velocity is assumed to be equivalent to the motion of the structural surface. Projecting the velocity normal to the structure gives the fluid-structure coupling: $\boldsymbol{v}\cdot\boldsymbol{n} = \boldsymbol{v}_s \cdot \boldsymbol{n}$ where $\boldsymbol{v}_s(\boldsymbol{x}\,,\,t)$ is the structural velocity vector. The influence of the fluid pressure acting on the structure is given by the normal traction $\boldsymbol{\sigma}\cdot\boldsymbol{n} = -p\boldsymbol{n}$ where $\boldsymbol{\sigma}$ is the symmetric Cauchy stress tensor. The stress is assumed to be related to the structural displacement vector $\boldsymbol{u}_s(\boldsymbol{x}\,,\,t)$ through a constitutive relation of the form:

$$\boldsymbol{\sigma} = \boldsymbol{C} : \nabla^s \boldsymbol{u}_s \tag{3}$$

where $\nabla^s \boldsymbol{u}_s$ is the symmetric gradient and $\boldsymbol{C} = \boldsymbol{C}(\boldsymbol{x})$ is the fourth-order tensor of elastic coefficients; assumed to satisfy the usual positive-definiteness (pointwise stability) and major and minor symmetry properties. The equations of motion for the structure are

$$\nabla \cdot \boldsymbol{\sigma} = \rho_s \dot{\boldsymbol{v}}_s \tag{4}$$

where $\rho_s = \rho_s(\boldsymbol{x}) > 0$ is the structural density, and $\boldsymbol{v}_s(\boldsymbol{x}\,,\,t) = \dot{\boldsymbol{u}}_s(\boldsymbol{x}\,,\,t)$.

The drivers for the problem are the initial conditions:

$$\boldsymbol{u}_s(\boldsymbol{x},0) = \boldsymbol{u}_s^0(\boldsymbol{x}), \quad \boldsymbol{x}\in\Omega_s \tag{5}$$

$$\boldsymbol{v}_s(\boldsymbol{x},0) = \boldsymbol{v}_s^0(\boldsymbol{x}), \quad \boldsymbol{x}\in\Omega_s \tag{6}$$

$$\phi(\boldsymbol{x},0) = \phi^0(\boldsymbol{x}), \quad \boldsymbol{x}\in\Omega_f \tag{7}$$

$$p(\boldsymbol{x},0) = p^0(\boldsymbol{x}), \quad \boldsymbol{x}\in\Omega_f \tag{8}$$

EXACT NON-REFLECTING BOUNDARY CONDITIONS

When domain based computational methods are used to model an infinite fluid region, a non-reflecting boundary must be introduced in the fluid at a finite distance from the submerged structure. Let the non-reflecting boundary be denoted Γ_∞ and positioned such that the original fluid region $\mathcal{B}$ is divided into a bounded interior domain Ω_f and an exterior domain Ω_∞ such that $\mathcal{B} = \Omega_f \cup \Omega_\infty$; see Fig. 1.

In the method presented, an exact non-reflecting boundary condition; derived in the frequency domain through a Fourier transform, is used as a basis for the space-time finite element formulation. An exact non-reflecting boundary condition is obtained by taking advantage of the fact that an outgoing wave solution can always be written in terms of a series of wave harmonics with respect to a separable coordinate system [25]. In the frequency domain, i.e., the time-harmonic problem, this idea has been exploited by several researchers to derive exact non-reflecting boundary conditions; see e.g. the Dirichlet-to-Neumann (DtN) impedance operator derived in [24]. The DtN operator is a nonlocal (integral) and frequency dependent boundary condition applied on a separable boundary Γ_∞.

For a spherical boundary Γ_∞ of radius $r = R$ in $\mathbb{R}^3$ with unit outward normal $\boldsymbol{n}$ to Γ_∞, the exact representation of the exterior acoustic impedance restricted to Γ_∞ is [24]:

$$\boldsymbol{v}(R,\theta,\varphi)\cdot\boldsymbol{n} = \sum_{n=0}^{\infty} z_n(\hat{k}) \int_{\Gamma_\infty} s_n(\theta,\varphi,\theta',\varphi')\ \phi(R,\theta',\varphi')\ d\Gamma' \tag{9}$$

where the DtN kernels $s_n,\ n = 0, 1, 2, \cdots$ are given by,

$$s_n = \sum_{j=0}^{n}{}' \alpha_{nj} P_n^j(\cos\varphi) P_n^j(\cos\varphi') \cos j(\theta - \theta') \quad (10)$$

$$\alpha_{nj} = \frac{(2n+1)(n-j)!}{2\pi R^2 (n+j)!} \quad (11)$$

with impedance coefficients,

$$z_n(\hat{k}) = \frac{k h_n'(\hat{k})}{h_n(\hat{k})} \quad (12)$$

In the above, $\omega > 0$ is the frequency, $k = \omega/c$ is the acoustic wavenumber, $\hat{k} = kR$ is a nondimensional wavenumber normalized with respect to the radial distance, $0 \le \theta < 2\pi$ is the circumferential angle and $0 \le \varphi < \pi$ is the polar angle for a spherical truncation boundary of radius $r = R$. The differential surface area is $d\Gamma = J_s d\theta d\varphi$, where $J_s = R^2 \sin\varphi$ is the surface Jacobian. The functions P_n^j are associated Legendre functions of the first kind, and h_n are spherical Hankel functions of the first kind of order n. The prime on h_n indicates differentiation with respect to its argument, and the prime after the sum indicates that a factor of $1/2$ multiplies the term with $j = 0$. The boundary condition (9) can be written in abstract operator form as,

$$\frac{\partial \phi}{\partial n}(\boldsymbol{x}\,,\, k) = \mathbb{S}(k)\ \phi(\boldsymbol{x}\,,\, k), \qquad \boldsymbol{x} \in \Gamma_\infty \quad (13)$$

relating Dirichlet data, ϕ, to Neumann data, $\partial\phi/\partial n = \boldsymbol{v}\cdot\boldsymbol{n}$, through the linear mapping $\mathbb{S}(k) : \phi \mapsto \partial\phi/\partial n$. For a spherical boundary the normal velocity specializes to a simple radial derivative: $\partial\phi/\partial n = \partial\phi/\partial r$.

A direct time-dependent counterpart to the DtN map can be obtained through a convolution integral in time as,

$$\boldsymbol{v}(\boldsymbol{x}\,,\, t)\cdot\boldsymbol{n} = \int_0^t \mathbb{S}(t-\tau)\phi(\tau)\ d\tau, \qquad \boldsymbol{x} \in \Gamma_\infty \quad (14)$$

resulting in a boundary condition that is non-local in both space and time dimensions. Implementation of (14) in a computational method requires storage of all previous solutions up to the current time step; a property that makes its use impractical for large-scale computations over long time intervals. Note that this limitation of the time convoluted DtN operator is also shared with the Kirchoff boundary integral representation.

In order to circumvent the difficulty of having to implement a temporal convolution integral, time-dependent boundary conditions are derived which replace the temporal integral with local temporal derivatives; see [17, 20]. Two alternative sequences were derived; the first retains the nonlocal spatial integral of the DtN map (9), while replacing the time-convolution in (14) with higher-order local time derivatives (local in time and nonlocal in space version), while the second involves only time and spatial derivatives (local in time and local in space version). In the following, some important results from the derivation are summarized.

Local in Time and Non-Local in Space Version

Consider the first two terms in the truncated DtN series; then (9) reduces to,

$$\boldsymbol{v}\cdot\boldsymbol{n} \quad = \quad z_0 \int_{\Gamma_\infty} \phi\, s_0\ d\Gamma' + z_1 \int_{\Gamma_\infty} \phi\, s_1\ d\Gamma' \quad (15)$$

Using the definition for $z_n(\hat{k})$ in (12) and relations

$$h_n(\hat{k}) = h_0(\hat{k}) \left[(-i)^n \sum_{j=0}^{n} \frac{(n+j)!}{j!(n-j)!} \left(\frac{-1}{2i\hat{k}}\right)^j \right], \quad (16)$$

for $n = 0, 1, 2, \cdots$, and

$$h_n(\hat{k})' = h_{n-1}(\hat{k}) - \left(\frac{n+1}{\hat{k}}\right) h_n(\hat{k}), \quad (17)$$

for $n = 1, 2, \cdots$, then (15) can be written in the alternative form,

$$\begin{aligned} \left(\frac{1}{R} - ik\right)\boldsymbol{v}\cdot\boldsymbol{n} \quad &= \quad \left(k^2 + \frac{2ik}{R} - \frac{1}{R^2}\right)\int_{\Gamma_\infty} \phi\, s_0\ d\Gamma' \\ &+ \quad \left(k^2 + \frac{2ik}{R} - \frac{2}{R^2}\right)\int_{\Gamma_\infty} \phi\, s_1\ d\Gamma' \end{aligned} \quad (18)$$

Direct application of the inverse Fourier transform gives the time-dependent counterpart:

$$\begin{aligned} K_f\,\boldsymbol{v}\cdot\boldsymbol{n} \quad &= \quad c^2 p_{,n} \\ &+ \quad \frac{1}{R}\int_{\Gamma_\infty} \left(R^2 p_{,t} + 2cRp - K_f\phi\right) s_0\ d\Gamma' \\ &+ \quad \frac{1}{R}\int_{\Gamma_\infty} \left(R^2 p_{,t} + 2cRp - 2K_f\phi\right) s_1\ d\Gamma' \end{aligned} \quad (19)$$

where the functions s_0 and s_1 are defined in (10). This time-dependent radiation boundary condition is perfectly absorbing for the first two spherical wave harmonics of order $n = 0$ and $n = 1$.

Similarly for the first three terms in (9), the local in time counterpart as reported in [17, 20] is

$$K_f\,\boldsymbol{v}\cdot\boldsymbol{n} = \frac{R}{3c}(6c^2p_{,n} + 4cRp_{,nt} + R^2p_{,ntt})$$

$$+\frac{1}{c_0}\int_{\Gamma_\infty}(c_1p_{,ttt} + c_2p_{,tt} + 10c_3p_{,t} + 9c_4p - 3c_5\phi)\,s_0\,d\Gamma^{'}$$

$$+\frac{1}{c_0}\int_{\Gamma_\infty}(c_1p_{,ttt} + c_2p_{,tt} + 11c_3p_{,t} + 12c_4p - 6c_5\phi)\,s_1\,d\Gamma^{'}$$

$$+\frac{1}{c_0}\int_{\Gamma_\infty}(c_1p_{,ttt} + c_2p_{,tt} + 13c_3p_{,t} + 18c_4p - 9c_5\phi)\,s_2\,d\Gamma^{'} \tag{20}$$

where

$$c_5 = c^2K_f; \qquad c_4 = c^3R$$
$$c_3 = c^2R^2; \qquad c_2 = 5cR^3$$
$$c_1 = R^4; \qquad c_0 = 3c^2R$$

This condition is perfectly absorbing for the first three spherical wave harmonics of order $n = 0, 1, 2$. These are nonlocal operators that involve a spatial integral yet retain the important property of locality in time. In general, the boundary operators in this sequence will have higher-order time derivatives which make them difficult to implement in standard finite element implementations. However, when implemented in the discontinuous space-time finite element formulation, standard $C^0(\Gamma_\infty \times I_n)$ continuous interpolations may be used on the radiation boundary in both the space and time dimensions [17, 20].

Local in Time and Local in Space Version

In [17, 20] it is shown that when the solution on the boundary Γ_∞ contains only a finite number of spherical harmonics, then (9) can be transformed into an exact condition which is local in both space $\boldsymbol{x}$ and time t. The transformation starts with the ideas of Givoli and Keller [26], where a spatially local counterpart to the nonlocal DtN map $\mathbb{S}$ was obtained for the two-dimensional Helmholtz equation. The extension to three-dimensions was given by Harari [27].

The sequence of local boundary conditions is obtained by truncating the DtN map given in (9), so that the sum over n extends over the finite range $n = 0, 1, \cdots N-1$, and expressing the first N terms in the DtN map as:

$$\boldsymbol{v}\cdot\boldsymbol{n} = \sum_{n=0}^{N-1} z_n(\hat{k})\,Y_n(\theta\,,\,\varphi) \tag{21}$$

where

$$Y_n(\theta\,,\,\varphi) = \sum_{j=0}^{n}{}' P_n^j(\cos\varphi)(A_{nj}\cos j\theta + B_{nj}\sin j\theta) \tag{22}$$

are spherical surface harmonics of order n, with nonlocal coefficients A_{nj} and B_{nj}. The initial goal is to replace the nonlocal spatial integrals embedded in the coefficients A_{nj} and B_{nj} with local spatial derivatives. This can be accomplished by recognizing that Y_n can be interpreted as eigenfunctions of the Laplace-Beltrami operator

$$\Delta_\Gamma := \frac{1}{\sin\varphi}\frac{\partial}{\partial\varphi}\left(\sin\varphi\frac{\partial}{\partial\varphi}\right) + \frac{1}{\sin^2\varphi}\frac{\partial^2}{\partial\theta^2} \tag{23}$$

with eigenvalues $\lambda = -n(n+1)$, so that

$$[n(n+1)]^m Y_n = (-\Delta_\Gamma)^m Y_n \tag{24}$$

This property of the spherical harmonics suggests writing the impedance coefficients as a series of powers of $n(n+1)$:

$$z_n(\hat{k}) = \sum_{m=0}^{N-1}[n(n+1)]^m\beta_m(\hat{k}), \qquad n = 0, 1, \cdots, N-1 \tag{25}$$

This is a system of N linear equations for the N unknown values $\beta_m, m = 0, 1, \cdots N$. Using (25) to replace z_n in (21) gives,

$$\boldsymbol{v}\cdot\boldsymbol{n} = \sum_{n=0}^{N-1}\sum_{m=0}^{N-1}\beta_m(\hat{k})\,[n(n+1)]^m\,Y_n(\theta\,,\,\varphi) \tag{26}$$

Now using (24) to replace $[n(n+1)]^mY_n$ with the high-order tangential derivatives $(-\Delta_\Gamma)^mY_n$, and using the assumption that the solution ϕ on Γ_∞ contains only the first N spherical harmonics, the following sequence of local radiation boundary conditions is obtained:

$$\boldsymbol{v}\cdot\boldsymbol{n} \quad = \quad \sum_{m=0}^{N-1}\beta_m(\hat{k})\,(-\Delta_\Gamma)^m\phi \qquad \text{on } \Gamma_\infty \tag{27}$$

where the values of $\beta_m(\hat{k})$ are obtained by solving the $N \times N$ linear algebraic system (25). Since this sequence follows directly from the truncated DtN map, these radiation boundary operators are exact for waves consisting of the first N spherical harmonics. In this case, the

nonlocal spatial integrals have been replaced by a linear map expressed in terms of the differential operator $(\Delta_\Gamma)^m$.

The next step is to obtain an exact local in time counterpart to (27) through an inverse Fourier transform. To this end use is made of the finite series expansion for the spherical Hankel functions embedded in the coefficients $\beta_m(\hat{k})$.

For the first two operators in the sequence corresponding to $N = 2$, the system (25) reduces to $\beta_0 = z_0$ and $\beta_1 = (z_1 - z_0)/2$, so that the local DtN condition (27) specializes to,

$$\boldsymbol{v} \cdot \boldsymbol{n} = z_0 \phi + \frac{1}{2}(z_0 - z_1)\Delta_\Gamma \phi \tag{28}$$

Clearing the common denominator $h_0 h_1$ and using the recurrence relation (17) in conjunction with (16) and after some algebraic manipulation, we obtain the simplified form,

$$\left(\frac{1}{R} - ik\right) \boldsymbol{v} \cdot \boldsymbol{n} = \left(k^2 + \frac{2ik}{R} - \frac{1}{R^2}\right)\phi + \frac{1}{2R^2}\Delta_\Gamma \phi \tag{29}$$

Since this expression involves only terms in powers of ik, the inverse Fourier transform is readily obtained with the desired result,

$$K_f \, \boldsymbol{v} \cdot \boldsymbol{n} = cRp_{,n} + Rp_{,t} + 2cp - \frac{K_f}{2R}(2 - \Delta_\Gamma)\phi \tag{30}$$

This second-order accurate local boundary condition is perfectly absorbing for the first two spherical wave harmonics of orders $n = 0$ and $n = 1$. Expressions for the exact time-dependent local boundary conditions for higher-order harmonics $N = 3, 4, \cdots$, involve higher-order temporal and tangential derivatives, and are obtained using the same procedure as indicated for $N = 1, 2$; see [17, 20].

This new sequence of local time-dependent boundary conditions provide increasing accuracy with order N which, however, is also a measure of the difficulty of implementation. In general, the Nth-order condition contains all the even tangential and temporal derivatives up to order $2(N-1)$. Because the time-discontinuous formulation allows for the use of C^0 interpolations to represent the high-order time derivatives, it is possible to implement this sequence of time-dependent absorbing boundary conditions up to any order desired [17, 20]. However for high-order operators in the sequence extending beyond $N \geq 3$, the lowest possible order of spatial continuity on the artificial boundary that can be achieved after integration by parts is C^{N-2}. For these high-order operators a layer of boundary elements adjacent to Γ_∞, possessing high-order tangential continuity on Γ_∞ are needed.

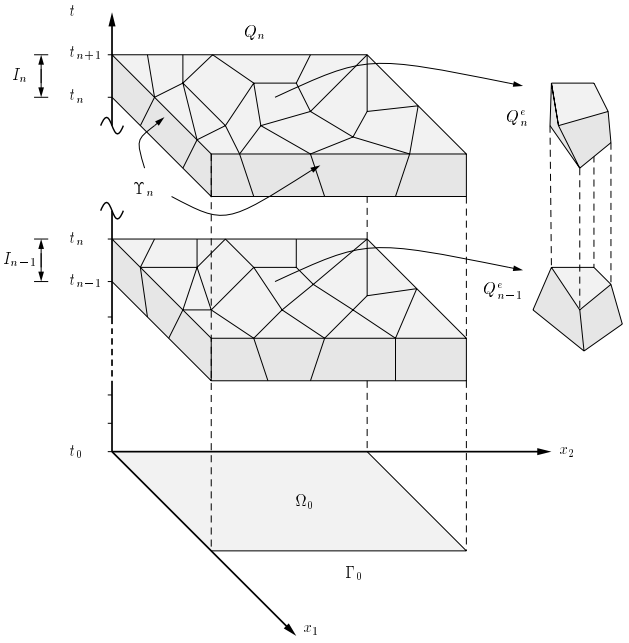

Fig. 2: Illustration of two consecutive space-time slabs with unstructured finite element meshes in space-time.

TIME-DISCONTINUOUS GALERKIN FINITE ELEMENT FORMULATION

The development of the space-time method proceeds by considering a partition of the time interval, $I =]0, T[$, of the form: $0 = t_0 < t_1 < \cdots < t_N = T$, with $I_n =]t_n, t_{n+1}[$ and $\Delta t_n = t_{n+1} - t_n$. Using this notation, $Q_n^s = \Omega_s \times I_n$, and $Q_n^f = \Omega_f \times I_n$ are the nth space-time slabs for the structure and fluid respectively. For the nth space-time slab, the spatial domain is subdivided into $(n_{el})_n$ elements, and the interior of the e^{th} element is defined as Q_n^e. Figure 2 shows an illustration of two consecutive space-time slabs Q_{n-1} and Q_n for the fluid where the superscript is omitted for clarity.

Within each space-time element, the trial solution and weighting function are approximated by polynomials in both $\boldsymbol{x}$ and t. These functions are assumed $C^0(Q_n)$ continuous throughout each space-time slab, but are allowed to be discontinuous across the interfaces of the slabs. An important component in the success of the space-time method is the incorporation of discontinuous temporal jump terms at each space-time slab interface; for a function w^h, the jump operator is defined as,

$$[\![w^h(t_n)]\!] \quad = \quad w^h(\boldsymbol{x}\,, t_n^+) \, - \, w^h(\boldsymbol{x}\,, t_n^-)$$

These jump operators weakly enforce initial conditions across time slabs and are crucial for obtaining an uncon-

ditionally stable algorithm for unstructured space-time finite element discretizations with high-order interpolations. This feature of the time-discontinuous method, allows for the general use of high-order elements and spectral-type interpolations in both space and time. The specific form of these jump operators are designed such that a natural norm emanates from the variational equation and satisfies a strong coercivity condition.

The space of finite element basis functions for the multi-field representation for the fluid are stated in terms of *independent* trial velocity potential ϕ^h, and trial pressure p^h, variables:

Trial velocity potential:

$$\mathcal{T}_1^h \quad = \quad \left\{ \phi^h \middle| \phi^h \in C^0(\bigcup_{n=0}^{N-1} Q_n^f)\,,\, \phi^h\Big|_{Q_n^{f^e}} \in \mathcal{P}^k(Q_n^{f^e}) \right\}$$

Trial pressure:

$$\mathcal{T}_2^h \quad = \quad \left\{ p^h \middle| p^h \in C^0(\bigcup_{n=0}^{N-1} Q_n^f)\,,\, p^h\Big|_{Q_n^{f^e}} \in \mathcal{P}^l(Q_n^{f^e}) \right\}$$

where $\mathcal{P}^k$ denotes the space of kth-order polynomials and C^0 denotes the space of continuous functions. The collections of finite element basis functions for the approximation to the structural equations are given by the spaces,

Trial structural displacements:

$$\mathcal{S}_1^h = \left\{ \boldsymbol{u}_s^h(\boldsymbol{x},t) \middle| \right.$$
$$\left. \boldsymbol{u}_s^h \in (C^0(\bigcup_{n=0}^{N-1} Q_n^s))^{n_{sd}}\,,\, \boldsymbol{u}_s^h\Big|_{Q_n^{s^e}} \in (\mathcal{P}^m(Q_n^{s^e}))^{n_{sd}} \right\}$$

Trial structural velocities:

$$\mathcal{S}_2^h = \left\{ \boldsymbol{v}_s^h(\boldsymbol{x},t) \middle| \right.$$
$$\left. \boldsymbol{v}_s^h \in (C^0(\bigcup_{n=0}^{N-1} Q_n^s))^{n_{sd}}\,,\, \boldsymbol{v}_s^h\Big|_{Q_n^{s^e}} \in (\mathcal{P}^n(Q_n^{s^e}))^{n_{sd}} \right\}$$

Before stating the space-time variational equations, it is useful to introduce the following notation.

$$\begin{aligned}
(\delta\boldsymbol{u}_s^h\,,\,\boldsymbol{u}_s^h)_{\Omega_s} &= \int_{\Omega_s} \delta\boldsymbol{u}_s^h \cdot \boldsymbol{u}_s^h \, d\Omega \\
a(\delta\boldsymbol{u}_s^h\,,\,\boldsymbol{u}_s^h)_{\Omega_s} &= \int_{\Omega_s} \nabla\delta\boldsymbol{u}_s^h \cdot \boldsymbol{\sigma}(\boldsymbol{u}_s^h) \, d\Omega \\
(\delta p^h\,,\,p^h)_{\Omega_f} &= \int_{\Omega_f} \delta p^h \, p^h \, d\Omega \\
(\delta p^h\,,\,p^h)_{\Gamma} &= \int_{\Gamma} \delta p^h \, p^h \, d\Gamma \\
(\delta p^h\,,\,p^h)_{Q_n} &= \int_{t_n}^{t_{n+1}} (\delta p^h\,,\,p^h)_{\Omega} \, dt \\
(\delta p^h\,,\,p^h)_{\Upsilon_n} &= \int_{t_n}^{t_{n+1}} (\delta p^h\,,\,p^h)_{\Gamma} \, dt
\end{aligned}$$

The meaning of other similar bilinear forms may be inferred from these. In the above definitions, a delta refers to the variation of the function, i.e. the corresponding weighting function. The L_2 norm is denoted by $||\phi||_\Omega = (\phi\,,\,\phi)_\Omega^{1/2}$.

MULTI-FIELD SPACE-TIME VARIATIONAL EQUATION

The multi-field space-time variational equation is obtained from a weighted residual of the governing equations and incorporates time-discontinuous jump terms. The specific form of this new formulation is designed such that unconditional stability for arbitrary space-time finite element discretizations can be proved through a functional analysis of the method. The statement of the time-discontinuous Galerkin method for the multi-field formulation is:

Within each space-time slab, $n = 0, 1, ..., N-1$;
Find $\boldsymbol{U}_f^h := \{\phi^h\,,\,p^h\} \in \mathcal{T}_1^h \times \mathcal{T}_2^h$
and $\boldsymbol{U}_s^h := \{\boldsymbol{u}_s^h\,,\,\boldsymbol{v}_s^h\} \in \mathcal{S}_1^h \times \mathcal{S}_2^h$,
such that for all weighting functions
$\delta\boldsymbol{U}_f^h := \{\delta\phi^h\,,\,\delta p\} \in \mathcal{T}_1^h \times \mathcal{T}_2^h$, and
$\delta\boldsymbol{U}_s^h := \{\delta\boldsymbol{u}_s^h\,,\,\delta\boldsymbol{v}_s^h\} \in \mathcal{S}_1^h \times \mathcal{S}_2^h$,
the following coupled variational equation is satisfied:

$$\begin{aligned}
& B_f(\delta\boldsymbol{U}_f^h\,,\,\boldsymbol{U}_f^h)_n \\
& + B_s(\delta\boldsymbol{U}_s^h\,,\,\boldsymbol{U}_s^h)_n \\
& + B_\infty(\delta\boldsymbol{U}_f^h\,,\,\boldsymbol{U}_f^h)_n \\
& - \left(\delta p^h\,,\,\boldsymbol{v}_s^h \cdot \boldsymbol{n}\right)_{(\Upsilon_i)_n} + \left(\delta\boldsymbol{v}_s^h \cdot \boldsymbol{n}\,,\,p^h\right)_{(\Upsilon_i)_n} \\
& \quad = \quad L_f(\delta\boldsymbol{U}_f^h)_n + L_s(\delta\boldsymbol{U}_s^h)_n
\end{aligned} \tag{31}$$

with the following definitions;

$$\begin{aligned} B_f(\delta \boldsymbol{U}_f^h\,,\,\boldsymbol{U}_f^h)_n \;&:=\; \big(\delta p^h\,,\,K_f^{-1}\dot{p}^h\big)_{Q_n^f} \\ &-\; (\nabla\delta p^h\,,\,\boldsymbol{v}^h)_{Q_n^f} \\ &+\; (\delta\boldsymbol{v}^h\,,\,\mathcal{L}_f\boldsymbol{U}_f^h)_{\tilde{Q}_n^f} \\ &+\; \big(\delta p^h(t_n^+)\,,\,K_f^{-1}p^h(t_n^+)\big)_{\Omega_f} \\ &+\; \big(\delta\boldsymbol{v}^h(t_n^+)\,,\,\rho_f\boldsymbol{v}^h(t_n^+)\big)_{\Omega_f} \end{aligned} \tag{32}$$

$$\begin{aligned} B_s(\delta \boldsymbol{U}_s^h\,,\,\boldsymbol{U}_s^h)_n \;&:=\; \big(\delta\boldsymbol{v}_s^h\,,\,\rho_s\dot{\boldsymbol{v}}_s^h\big)_{Q_n^s} \\ &+\; a(\delta\boldsymbol{v}_s^h\,,\,\boldsymbol{u}_s^h)_{Q_n^s} \\ &+\; a(\delta\boldsymbol{u}_s^h\,,\,\mathcal{L}_s\boldsymbol{U}_s^h)_{\tilde{Q}_n^s} \\ &+\; \big(\delta\boldsymbol{v}_s^h(t_n^+)\,,\,\rho_s\boldsymbol{v}_s^h(t_n^+)\big)_{\Omega_s} \\ &+\; a\big(\delta\boldsymbol{u}_s^h(t_n^+)\,,\,\boldsymbol{u}_s^h(t_n^+)\big)_{\Omega_s} \end{aligned} \tag{33}$$

$$\begin{aligned} L_f(\delta \boldsymbol{U}_f^h)_n \;&:=\; \big(\delta p^h(t_n^+)\,,\,K_f^{-1}p^h(t_n^-)\big)_{\Omega_f} \\ &+\; \big(\delta\boldsymbol{v}^h(t_n^+)\,,\,\rho_f\boldsymbol{v}^h(t_n^-)\big)_{\Omega_f} \end{aligned} \tag{34}$$

$$\begin{aligned} L_s(\delta \boldsymbol{U}_s^h)_n \;&:=\; \big(\delta\boldsymbol{v}_s^h(t_n^+)\,,\,\rho_s\boldsymbol{v}_s^h(t_n^-)\big)_{\Omega_s} \\ &+\; a\big(\delta\boldsymbol{u}_s^h(t_n^+)\,,\,\boldsymbol{u}_s^h(t_n^-)\big)_{\Omega_s} \end{aligned} \tag{35}$$

in which $\boldsymbol{v}^h = \nabla\phi^h$, $\delta\boldsymbol{v}^h = \nabla\delta\phi^h$, and

$$\mathcal{L}_f\boldsymbol{U}_f^h \;=\; \rho_f\dot{\boldsymbol{v}}^h + \nabla p^h \tag{36}$$

$$\mathcal{L}_s\boldsymbol{U}_s^h \;=\; \dot{\boldsymbol{u}}_s^h - \boldsymbol{v}_s^h \tag{37}$$

In the above expressions, a tilde refers to integration over element interiors. Note that the linear form $L_s(\cdot)_0$ is obtained from the general expression for $L_s(\cdot)_n$ by setting $n = 0$ and replacing $\boldsymbol{u}_s^h(0^-)$ by $\boldsymbol{u}_s^0$ and $\boldsymbol{v}_s^h(0^-)$ by $\boldsymbol{v}_s^0$. Likewise, $L_f(\cdot)_0$ is obtained by setting $n = 0$ in (35) and replacing $\phi^h(0^-)$ and $p^h(0^-)$ with the initial conditions given in (8). $B_f(\cdot\,,\,\cdot)_n$ and $B_s(\cdot\,,\,\cdot)_n$ are bilinear forms for the fluid and structure respectively. Fluid-structure interaction is accomplished through the coupling operators defined on the fluid-structure interface $(\Upsilon_i)_n := \Gamma_i \times I_n$. The operator B_∞, incorporates the time-dependent radiation boundary conditions on the fluid truncation boundary Γ_∞. The definition of this operator depends on the order of the spatial and/or temporal derivatives appearing in the radiation boundary condition and will be described later. The method is applied in one space-time slab at a time; data from the end of the previous slab are employed as initial conditions for the current slab; i.e., the solution is obtained for a given time interval T and time step Δt_n by solving the variational equation (31) in order for each $n = 0, 1, 2, \ldots N-1$.

As a result of being a weighted residual based formulation, the method presented is *consistent* in the sense that for a sufficiently smooth exact solution to the initial/boundary-value problem (1) – (8), with a non-reflecting boundary condition of the form (19), (20), or (30), $\boldsymbol{U}_f = \{\phi\,,\,p\}$ and $\boldsymbol{U}_s = \{\boldsymbol{u}_s\,,\,\boldsymbol{v}_s\}$; where $p = -\rho_f\dot{\phi}$ and $\boldsymbol{v}_s = \dot{\boldsymbol{u}}_s$, satisfies,

$$\begin{aligned} &B_f(\delta\boldsymbol{U}_f^h\,,\,\boldsymbol{U}_f)_n \\ &+B_s(\delta\boldsymbol{U}_s^h\,,\,\boldsymbol{U}_s)_n \\ &+B_\infty(\delta\boldsymbol{U}_f^h\,,\,\boldsymbol{U}_f)_n \\ &-\big(\delta p^h\,,\,\boldsymbol{v}_s\cdot\boldsymbol{n}\big)_{(\Upsilon_i)_n} + \big(\delta\boldsymbol{v}_s^h\cdot\boldsymbol{n}\,,\,p\big)_{(\Upsilon_i)_n} \\ &\quad=\; L_f(\delta\boldsymbol{U}_f^h)_n + L_s(\delta\boldsymbol{U}_s^h)_n \end{aligned} \tag{38}$$

$\forall\ \delta\boldsymbol{U}_f^h \in \mathcal{T}_1^h \times \mathcal{T}_2^h$, and $\delta\boldsymbol{U}_s^h \in \mathcal{S}_1^h \times \mathcal{S}_2^h$ and $n = 0, 1, ..., N-1$. Consequently,

$$\begin{aligned} &B_f(\delta\boldsymbol{U}_f^h\,,\,\boldsymbol{E}_f)_n + B_s(\delta\boldsymbol{U}_s^h\,,\,\boldsymbol{E}_s)_n + B_\infty(\delta\boldsymbol{U}_f^h\,,\,\boldsymbol{E}_f)_n \\ &-\big(\delta p^h\,,\,(\boldsymbol{v}_s^h - \boldsymbol{v}_s)\cdot\boldsymbol{n}\big)_{(\Upsilon_i)_n} + \big(\delta\boldsymbol{v}_s^h\cdot\boldsymbol{n}\,,\,p^h - p\big)_{(\Upsilon_i)_n} = 0 \end{aligned} \tag{39}$$

where $\boldsymbol{E}_f = \boldsymbol{U}_f^h - \boldsymbol{U}_f$ and $\boldsymbol{E}_s = \boldsymbol{U}_s^h - \boldsymbol{U}_s$ is the error; in components $\boldsymbol{E}_f = \{\phi^h - \phi\,,\,p^h - p\}$ and $\boldsymbol{E}_s = \{\boldsymbol{u}_s^h - \boldsymbol{u}_s\,,\,\boldsymbol{v}_s^h - \boldsymbol{v}_s\}$. This formal consistency of (31) with the strong (local) form of the problem is necessary for maintaining optimal convergence rates for higher-order basis functions.

A natural measure of stability for the coupled structural acoustics problem is the *total energy* for the system:

$$\mathbb{E}(\boldsymbol{U}_f\,,\,\boldsymbol{U}_s) := \mathcal{E}_f(\boldsymbol{U}_f) + \mathcal{E}_s(\boldsymbol{U}_s) \tag{40}$$

$$\mathcal{E}_s(\boldsymbol{U}_s) \;=\; \frac{1}{2}\,(\boldsymbol{v}_s\,,\,\rho_s\boldsymbol{v}_s)_{\Omega_s} \;+\; \frac{1}{2}\,a(\boldsymbol{u}_s\,,\,\boldsymbol{u}_s)_{\Omega_s} \tag{41}$$

$$\mathcal{E}_f(\boldsymbol{U}_f) \;=\; \frac{1}{2}\,||K_f^{-1/2}\,p||_{\Omega_f}^2 \;+\; \frac{1}{2}\,||\rho_f^{1/2}\boldsymbol{v}||_{\Omega_f}^2 \tag{42}$$

where $\mathcal{E}_f$ and $\mathcal{E}_s$ denote the energy for the acoustic fluid and elastic structure respectively.

Stability, or *coercivity*, is established as follows:

$$\begin{aligned} B_f(\boldsymbol{U}_f^h\,,\,\boldsymbol{U}_f^h)_n &= (p^h\,,\,K_f^{-1}\dot{p}^h)_{Q_n^f} + (\boldsymbol{v}^h\,,\,\rho_f\dot{\boldsymbol{v}}^h)_{Q_n^f} \\ &\quad + 2\mathcal{E}_f(\boldsymbol{U}_f^h(t_n^+)) \\ &= \mathcal{E}_f(\boldsymbol{U}_f^h(t_{n+1}^-)) + \mathcal{E}_f(\boldsymbol{U}_f^h(t_n^+)) \quad (43) \end{aligned}$$

Similarly,

$$\begin{aligned} B_s(\boldsymbol{U}_s^h\,,\,\boldsymbol{U}_s^h)_n &= (\boldsymbol{v}_s^h\,,\,\rho_s\dot{\boldsymbol{v}}_s^h)_{Q_n^s} + a(\boldsymbol{u}_s^h\,,\,\dot{\boldsymbol{u}}_s^h)_{Q_n^s} \\ &\quad + 2\mathcal{E}_s(\boldsymbol{U}_s^h(t_n^+)) \\ &= \mathcal{E}_s(\boldsymbol{U}_s^h(t_{n+1}^-)) + \mathcal{E}_s(\boldsymbol{U}_s^h(t_n^+)) \quad (44) \end{aligned}$$

Then

$$\begin{aligned} B_f(\boldsymbol{U}_f^h\,,\,\boldsymbol{U}_f^h)_n &+ B_s(\boldsymbol{U}_s^h\,,\,\boldsymbol{U}_s^h)_n - \big(p^h\,,\,\boldsymbol{v}_s^h\cdot\boldsymbol{n}\big)_{(\Upsilon_i)_n} \\ &\quad + \big(\boldsymbol{v}_s^h\cdot\boldsymbol{n}\,,\,p^h\big)_{(\Upsilon_i)_n} \\ &= \mathcal{E}_f(\boldsymbol{U}_f^h(t_{n+1}^-)) + \mathcal{E}_f(\boldsymbol{U}_f^h(t_n^+)) \\ &\quad + \mathcal{E}_s(\boldsymbol{U}_s^h(t_{n+1}^-)) + \mathcal{E}_s(\boldsymbol{U}_s^h(t_n^+)) \\ &= \mathbb{E}(t_{n+1}^-) + \mathbb{E}(t_n^+) \quad (45) \end{aligned}$$

This is the *coercivity condition.*
Furthermore,

$$\begin{aligned} L_f(\boldsymbol{U}_f^h)_n &= (p^h(t_n^+)\,,\,K_f^{-1}p^h(t_n^-)_{\Omega_f} \\ &\quad + (\boldsymbol{v}^h(t_n^+)\,,\,\rho_f\boldsymbol{v}^h(t_n^-))_{\Omega_f} \\ &\le \mathcal{E}_f(\boldsymbol{U}_f^h(t_n^+)) + \mathcal{E}_f(\boldsymbol{U}_f^h(t_n^-)) \quad (46) \end{aligned}$$

and

$$L_s(\boldsymbol{U}_s^h)_n \le \mathcal{E}_s(\boldsymbol{U}_s^h(t_n^+)) + \mathcal{E}_s(\boldsymbol{U}_s^h(t_n^-)) \quad (47)$$

so that

$$L_f(\boldsymbol{U}_f^h)_n + L_s(\boldsymbol{U}_s^h)_n \le \mathbb{E}(t_n^+) + \mathbb{E}(t_n^-) \quad (48)$$

Finally, setting $\delta\boldsymbol{U}_f^h = \boldsymbol{U}_f^h$, $\delta\boldsymbol{U}_s^h = \boldsymbol{U}_s^h$ in (31), and using (45) and (48) gives the stability condition:

$$\mathbb{E}(t_{n+1}^-) + B_\infty(\boldsymbol{U}_f^h\,,\,\boldsymbol{U}_f^h)_n \le \mathbb{E}(t_n^-), \quad \forall\ \Delta t_n > 0, \quad (49)$$

and $n = 0, 1, \ldots N-1$. Eq. (49) states that the computed total energy for the system plus the radiation energy absorbed through the artificial boundary at the end of a time step is always less than or equal to the total energy at the previous time step for arbitrary step sizes. This result implies that *the space-time formulation presented is unconditionally stable.*

Matrix equations are obtained by introducing space-time finite element approximations for the independent variables:

$$\begin{aligned} \phi^h(\boldsymbol{x}\,,\,t) &= \boldsymbol{N}_f(\boldsymbol{x}\,,\,t)\boldsymbol{\phi}, \qquad (\boldsymbol{x}\,,\,t) \in Q_n^f \quad (50) \\ p^h(\boldsymbol{x}\,,\,t) &= \boldsymbol{\chi}_f(\boldsymbol{x}\,,\,t)\boldsymbol{p}, \qquad (\boldsymbol{x}\,,\,t) \in Q_n^f \quad (51) \\ \boldsymbol{u}_s^h(\boldsymbol{x}\,,\,t) &= \boldsymbol{N}_s(\boldsymbol{x}\,,\,t)\boldsymbol{d}, \qquad (\boldsymbol{x}\,,\,t) \in Q_n^s \quad (52) \\ \boldsymbol{v}_s^h(\boldsymbol{x}\,,\,t) &= \boldsymbol{\chi}_s(\boldsymbol{x}\,,\,t)\boldsymbol{c}, \qquad (\boldsymbol{x}\,,\,t) \in Q_n^s \quad (53) \end{aligned}$$

with their associated weighting (variational) parameters. In these expressions $\{\boldsymbol{N}_f\,,\,\boldsymbol{N}_s\} \in \mathcal{T}_1^h \times \mathcal{S}_1^h$ and $\{\boldsymbol{\chi}_f\,,\,\boldsymbol{\chi}_s\} \in \mathcal{T}_2^h \times \mathcal{S}_2^h$ are matrices defining global basis functions over a space-time slab, and $\{\boldsymbol{\phi}\,,\,\boldsymbol{p}\}$ and $\{\boldsymbol{d}\,,\,\boldsymbol{c}\}$ are global solution vectors. Inserting (50) – (53) into the variational equation (31) leads to the coupled system of algebraic equations to be solved in sequence for each time interval $I_n =]t_n\,,\,t_{n+1}[,\ n = 0, 1, \cdots N-1$:

$$\begin{bmatrix} \boldsymbol{K}_f & \boldsymbol{C}_f & \boldsymbol{0} & \boldsymbol{0} \\ \boldsymbol{C}_f^T & \boldsymbol{M}_f & \boldsymbol{A} & \boldsymbol{0} \\ \boldsymbol{0} & \boldsymbol{A}^T & \boldsymbol{M}_s & \boldsymbol{C}_s \\ \boldsymbol{0} & \boldsymbol{0} & \boldsymbol{C}_s^T & \boldsymbol{K}_s \end{bmatrix} \begin{Bmatrix} \boldsymbol{\phi} \\ \boldsymbol{p} \\ \boldsymbol{c} \\ \boldsymbol{d} \end{Bmatrix} = \begin{Bmatrix} \boldsymbol{f}_f^1 \\ \boldsymbol{f}_f^2 \\ \boldsymbol{f}_s^2 \\ \boldsymbol{f}_s^1 \end{Bmatrix} \quad (54)$$

where $\boldsymbol{K}_s\,,\,\boldsymbol{M}_s$ are global matrices emanating from the structural bilinear operator B_s, and $\boldsymbol{K}_f\,,\,\boldsymbol{M}_f$ are global matrices emanating from the fluid bilinear operator B_f and B_∞; C_f is the coupling matrix relating acoustic pressure and velocity potential solution arrays; likewise C_s is the coupling matrix relating structural displacement and velocity degrees-of-freedom; $\boldsymbol{A}$ is the fluid-structure coupling matrix defined as:

$$\boldsymbol{A}^T = \int_{t_n}^{t_{n+1}} \int_{\Gamma_i} \boldsymbol{\chi}_s^T\,\boldsymbol{n}\,\boldsymbol{\chi}_f\ d\Gamma\ dt \quad (55)$$

Note that *the coupled matrix system is positive-definite.* The positive form of (54) follows directly from the stability (coercivity) result (45).

Implementation of Local High-Order Accurate Non-Reflecting Boundary Conditions

A direct approach in which to implement time-dependent boundary conditions is to define a linear operator $\mathbb{S}_m$ as,

$$\boldsymbol{v}\cdot\boldsymbol{n} - \mathbb{S}_m(\boldsymbol{U}_f) = 0 \quad (56)$$

which implies

$$\boldsymbol{v}\cdot\boldsymbol{n} = \mathbb{S}_m(\boldsymbol{U}_f) \qquad \text{on}\ \ \Gamma_\infty \quad (57)$$

For example, the first three local in space and time operators $\mathbb{S}_m$ for m equal to 1,2 and 3 are [17, 18, 20]:

$$\mathbb{S}_1(\boldsymbol{U}_f) = -\frac{1}{R}\phi + \frac{1}{\rho_f c}p \tag{58}$$

$$\mathbb{S}_2(\boldsymbol{U}_f) = -\frac{1}{2R}(2-\Delta_\Gamma)\phi + \frac{1}{\rho_f c}\left(2 + R\frac{\partial}{\partial r}\right)p + \frac{R}{K_f}p_{,t} \tag{59}$$

$$\begin{aligned}\mathbb{S}_3(\boldsymbol{U}_f) = & -\frac{1}{24R}(24 - 14\Delta_\Gamma - (\Delta_\Gamma)^2)\phi \\ & + \frac{1}{2\rho_f c}\left(6 - \Delta_\Gamma + 4R\frac{\partial}{\partial r}\right)p \\ & + \frac{R}{6K_f}\left(20 - \Delta_\Gamma + 8R\frac{\partial}{\partial r}\right)p_{,t} \\ & + \frac{R^2}{3K_f c}\left(5 + R\frac{\partial}{\partial r}\right)p_{,tt} \\ & + \frac{R^3}{3K_f c^2}p_{,ttt}\end{aligned} \tag{60}$$

These boundary conditions are incorporated into the finite element method as a natural boundary condition, i.e., they are enforced weakly in both time and space. For example, the operator defined on Γ_∞ in Eq. (31) for the local second-order boundary condition (59) is given by:

$$\begin{aligned}B_\infty(\delta\boldsymbol{U}_f^h\,,\,\boldsymbol{U}_f^h)_n = & \ (\delta p^h\,,\,\mathbb{S}_2(\boldsymbol{U}_f^h))_{(\Upsilon_\infty)_n} \\ & + d_2\big(\delta p^h(t_n^+)\,,\,[\![p^h(t_n)]\!]\big)_{(\Upsilon_\infty)_n} \\ & + d_0\big(\delta\phi^h(t_n^+)\,,\,\rho_f[\![\phi^h(t_n)]\!]\big)_{(\Upsilon_\infty)_n}.\end{aligned} \tag{61}$$

where

$$\begin{aligned}\big(\delta p^h\,,\,\mathbb{S}_2(\boldsymbol{U}_f^h)\big)_{(\Upsilon_\infty)_n} = & \ d_2\big(\delta p^h\,,\,\dot{p}^h\big)_{(\Upsilon_\infty)_n} \\ & + d_1\big(\delta p^h\,,\,p^h\big)_{(\Upsilon_\infty)_n} \\ & - d_0\big(\delta p^h\,,\,\phi^h\big)_{(\Upsilon_\infty)_n} \\ & + d_0\big(\delta\phi^h\,,\,p^h + \rho_f\dot{\phi}^h\big)_{(\Upsilon_\infty)_n};\end{aligned} \tag{62}$$

$$\begin{aligned}d_0\big(\delta p^h\,,\,\phi^h\big)_{(\Upsilon_\infty)_n} := & \ \frac{1}{R}\big(\delta p^h\,,\,\phi^h\big)_{(\Upsilon_\infty)_n} \\ & + \frac{1}{2R}\big(\delta p^h_{,\varphi}\,,\,\phi^h_{,\varphi}\big)_{(\Upsilon_\infty)_n} \\ & + \frac{1}{2R}\big(\delta p^h_{,\theta}\,,\,\csc^2(\varphi)\,\phi^h_{,\theta}\big)_{(\Upsilon_\infty)_n}\end{aligned} \tag{63}$$

$$d_1\big(\delta p^h\,,\,p^h\big)_{(\Upsilon_\infty)_n} := \frac{2}{\rho_f c}\big(\delta p^h\,,\,p^h\big)_{(\Upsilon_\infty)_n} + \frac{R}{\rho_f c}\big(\delta p^h\,,\,p^h_{,r}\big)_{(\Upsilon_\infty)_n} \tag{64}$$

$$d_2\big(\delta p^h\,,\,\dot{p}^h\big)_{(\Upsilon_\infty)_n} := \frac{R}{K_f}\big(\delta p^h\,,\,\dot{p}^h\big)_{(\Upsilon_\infty)_n} \tag{65}$$

Note that integration-by-parts has been used to relax the continuity implied by the second-order tangential derivatives appearing in Δ_Γ from $C^1(\Gamma_\infty)$ to $C^0(\Gamma_\infty)$. The form of the terms defined in (61) involving temporal jump operators evaluated on the boundary Γ_∞, can be inferred from (63) and (65). These consistent jump terms act to weakly enforce continuity of $\boldsymbol{U}_f^h$ between space-time-slabs at the boundary Γ_∞. These additional operators are needed in order to ensure unconditional stability for the solution and are the crucial element that enable generalization of the time-discontinuous space-time finite element method to handle unbounded domains.

SINGLE-FIELD FORMULATION

If the finite element approximation for the acoustic pressure is selected such that, $p^h = -\rho_f\dot{\phi}^h$, which implies that the residual $\mathcal{L}_f\boldsymbol{U}_f^h = \rho_f\nabla\dot{\phi}^h + \nabla p^h = 0$, and similarly if the structural velocity is the time derivative of the structural displacement, $\boldsymbol{v}_s^h = \dot{\boldsymbol{u}}_s^h$, then the multi-field formulation (31) specializes to the single-field formulation derived in [17, 18, 20]. This simplification occurs when the temporal order of approximation for p^h and $\boldsymbol{v}_s^h$ is one order less than that used for ϕ^h and $\boldsymbol{u}_s^h$, respectively; i.e., $\{\boldsymbol{\chi}_f\,,\,\boldsymbol{\chi}_s\} = \{\boldsymbol{N}_{f,t}\,,\,\boldsymbol{N}_{s,t}\}$. In this case (31) becomes:
For $n = 0, 1, ..., N-1$; Find $\phi^h \in \mathcal{T}_1^h$ and $\boldsymbol{u}_s^h \in \mathcal{S}_1^h$,

such that $\forall\ \ \delta\phi^h \in \mathcal{T}_1^h$, and $\delta \boldsymbol{u}_s^h \in \mathcal{S}_1^h$:

$$\begin{aligned} & b_f(\delta\phi^h\,,\,\phi^h)_n \\ & +b_s(\delta \boldsymbol{u}_s^h\,,\,\boldsymbol{u}_s^h)_n \\ & +b_\infty(\delta\phi^h\,,\,\phi^h)_n \\ & +\big(\delta\dot{\phi^h}\,,\,\rho_f\dot{\boldsymbol{u}}_s^h\cdot\boldsymbol{n}\big)_{(\Upsilon_i)_n} \\ & -\big(\delta\dot{\boldsymbol{u}}_s\cdot\boldsymbol{n}\,,\,\rho_f\dot{\phi^h}\big)_{(\Upsilon_i)_n} \\ = \;& l_f(\delta\phi^h)_n + l_s(\delta\boldsymbol{u}_s^h)_n \end{aligned} \tag{66}$$

with the following definitions; $a = c^{-1}$,

$$\begin{aligned} b_f(\delta\phi^h\,,\,\phi^h)_n \;:=\; & \big(\delta\dot{\phi^h}\,,\,a^2\,\rho_f\ddot{\phi^h}\big)_{Q_n^f} \\ +\; & (\delta\dot{\boldsymbol{v}}^h\,,\,\rho_f\boldsymbol{v}^h)_{Q_n^f} \\ +\; & \big(\delta\dot{\phi^h}(t_n^+)\,,\,a^2\,\rho_f\dot{\phi^h}(t_n^+)\big)_{\Omega_f} \\ +\; & \big(\delta\boldsymbol{v}^h(t_n^+)\,,\,\rho_f\boldsymbol{v}^h(t_n^+)\big)_{\Omega_f} \end{aligned} \tag{67}$$

$$\begin{aligned} b_s(\delta\boldsymbol{u}_s^h\,,\,\boldsymbol{u}_s^h)_n \;:=\; & \big(\delta\dot{\boldsymbol{u}}_s^h\,,\,\rho_s\ddot{\boldsymbol{u}}_s^h\big)_{Q_n^s} \\ +\; & a(\delta\dot{\boldsymbol{u}}_s^h\,,\,\boldsymbol{u}_s^h)_{Q_n^s} \\ & +\big(\delta\dot{\boldsymbol{u}}_s^h(t_n^+)\,,\,\rho_s\dot{\boldsymbol{u}}_s^h(t_n^+)\big)_{\Omega_s} \\ & +a\big(\delta\boldsymbol{u}_s^h(t_n^+)\,,\,\boldsymbol{u}_s^h(t_n^+)\big)_{\Omega_s} \end{aligned} \tag{68}$$

$$\begin{aligned} l_f(\delta\phi^h)_n \;:=\; & \big(\delta\dot{\phi^h}(t_n^+)\,,\,a^2\,\rho_f\dot{\phi^h}(t_n^-)\big)_{\Omega_f} \\ & +\big(\delta\boldsymbol{v}^h(t_n^+)\,,\,\rho_f\boldsymbol{v}^h(t_n^-)\big)_{\Omega_f} \end{aligned}$$

$$\begin{aligned} l_s(\delta\boldsymbol{u}_s^h)_n \;:=\; & \big(\delta\dot{\boldsymbol{u}}_s^h(t_n^+)\,,\,\rho_s\dot{\boldsymbol{u}}_s^h(t_n^-)\big)_{\Omega_s} \\ & +a\big(\delta\boldsymbol{u}_s^h(t_n^+)\,,\,\boldsymbol{u}_s^h(t_n^-)\big)_{\Omega_s} \end{aligned} \tag{69}$$

The form of $b_\infty(\cdot\,,\,\cdot)_n$ follows directly from the definition of $B_\infty(\cdot\,,\,\cdot)_n$ with p^h replaced with $-\rho_f\dot{\phi^h}$. Using approximations (50) and (52) the matrix equations emanating from (66) take the form:

$$\left[\begin{array}{cc} \boldsymbol{k}_f & \boldsymbol{a} \\ \boldsymbol{a}^T & \boldsymbol{k}_s \end{array}\right]\left\{\begin{array}{c} \boldsymbol{\phi} \\ \boldsymbol{d} \end{array}\right\} = \left\{\begin{array}{c} \boldsymbol{f}_f \\ \boldsymbol{f}_s \end{array}\right\}, \tag{70}$$

for $n = 0, 1, \cdots N-1$, where $\boldsymbol{k}_s$ is the global matrix emanating from the structural operator b_s, and $\boldsymbol{k}_f$ is the global matrix emanating from the fluid operator b_f and b_∞, and $\boldsymbol{a}$ is the fluid-structure coupling matrix defined as

$$\boldsymbol{a}^T \;=\; \int_{t_n}^{t_{n+1}}\int_{\Gamma_i}\rho_f\boldsymbol{N}_{s,t}^T\boldsymbol{n}\boldsymbol{N}_{f,t}\;d\Gamma\;dt \tag{71}$$

In this expression, a subscript comma t denotes partial derivatives with respect to time and $\boldsymbol{N}_s(\boldsymbol{x},t) \in \mathcal{S}_1$ and $\boldsymbol{N}_f(\boldsymbol{x},t) \in \mathcal{T}_1$ are global shape function matrices representing the space-time finite element approximation to the structural displacement and acoustic velocity potential respectively. Since the single-field formulation is a special case of the multi-field formulation, the reduced matrix system defined in (70) is also positive-definite – a detailed proof is given in [21]. Secondary variables are obtained from postprocessing; i.e., $p^h = -\rho_f\dot{\phi^h} = -\rho_f\boldsymbol{N}_{f,t}\boldsymbol{\phi}$ and $\boldsymbol{v}_s^h = \dot{\boldsymbol{u}}_s^h = \boldsymbol{N}_{s,t}\boldsymbol{d}$.

GALERKIN LEAST-SQUARES STABILIZATION

For additional stability, local residuals of the governing differential equations in the form of least-squares may be added to the Galerkin variational equations. The Galerkin Least Squares (GLS) addition to the single-field variational equation for the fluid, (67) takes the form [17]:

$$\begin{aligned} b_{GLS}^f(\delta\phi^h\,,\,\phi^h)_n \;=\; & b_f(\delta\phi^h\,,\,\phi^h)_n \\ +\; & (K_f\tau\mathcal{L}\delta\phi^h\,,\,\mathcal{L}\phi^h)_{\tilde{Q}_n^f} \\ +\; & (K_f s[\![\delta\boldsymbol{v}(\boldsymbol{x})]\!]\cdot\boldsymbol{n}\,,\,[\![\boldsymbol{v}(\boldsymbol{x})]\!]\cdot\boldsymbol{n})_{(\tilde{\Upsilon}^e)_n} \end{aligned} \tag{72}$$

where the residual $\mathcal{L}\phi^h = \nabla\cdot\nabla\phi^h - a^2\ddot{\phi^h}$ is the acoustic wave equation, and τ and s are local mesh parameters designed to improve desirable high frequency numerical dissipation without degrading the accuracy of the underlying time-discontinuous Galerkin method. Galerkin Least Squares methods have also been used to enhance the stability and accuracy of solutions to the related reduced wave equation (Helmholtz equation) governing time-harmonic acoustics in the frequency domain; see e.g. [27, 28], and [29, 30, 17].

ACCURACY ANALYSIS

Convergence rates for the simplified formulation have been determined in [17, 19]. Important results are that for the operator $\mathbb{S}_1$, defined in (58), and the time-discontinuous Galerkin Least Squares formulation, the

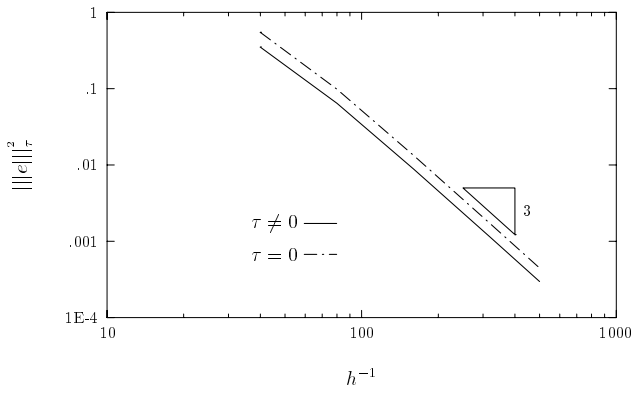

Fig. 3: Convergence of the numerical error employing a biquadratic space-time element. Results confirm the cubic rate of convergence predicted by the error estimate; i.e., $(2k-1) = 3$ for quadratic interpolation $k = 2$.

approximation error $\boldsymbol{E} = \{\phi^h - \phi\,,\, \boldsymbol{u}_s^h - \boldsymbol{u}_s\}$, converges at the rate

$$|||\boldsymbol{E}|||^2 \quad \leq \quad c(\phi)\, h_f^{2k-1} \,+\, c(\boldsymbol{u})\, h_s^{2m-1} \qquad (73)$$

where $h_s = \max\{c_L \Delta t\,,\, \Delta x\}$, and $h_f = \max\{c\Delta t\,,\, \Delta x\}$ are element mesh size parameters, c_L is the dilatational wave speed in Ω_s and c is the acoustic wave speed in Ω_f; Δx and Δt are maximum element diameters in space and time, respectively; $c(\boldsymbol{u})$ and $c(\phi)$ are values that are independent of h_s, h_f. The integers k and m are the finite element interpolation orders for the fluid and structure respectively. The norm $|||\boldsymbol{E}|||$ in which convergence is measured emanates naturally from the coupled fluid-structure variational equation (66) together with the least-squares operators. This result indicates that the error for the coupled system is controlled by the convergence rates in both the structure and the fluid; i.e., for an accurate solution to the coupled fluid-structure problem, discretizations for both the structural domain and the fluid domain must be adequately resolved. Accuracy can be increased in both space and time by simply increasing the order of the polynomial used in the finite element approximation. These convergence rates were verified numerically in [17, 19] for a model problem in one space dimension; both Galerkin and GLS formulations converge at the same rate as expected; see Fig. 3

NUMERICAL EXAMPLES

A few numerical results are presented to demonstrate the effectiveness of the space-time method to accurately model transient radiation and scattering from geometrically complex surfaces. Further details and a number of other examples may be found in [17, 18, 20, 21]. In Figures 4 – 5 results are presented for a pulsating sphere. These results illustrate the nearly perfect absorption of radiation energy through the non-reflecting boundary Γ_∞ using the local second-order operator $\mathbb{S}_2$ for a propagating wave pulse striking the boundary at severe angles of incidence. In Figures 6 and 7, results are presented for the transient scattering from a rigid cylinder with conical-to-spherical end caps and a large length-to-diameter ratio. This example represents a challenging problem where the multiple-scales involving the ratio of the wavelength to cylinder diameter and cylinder length dimension play a critical role in the complexity of the resulting scattered wave field. The numerical simulation starts with an initial pulse at $t = 3$. At $t = 6$ the incident pulse has expanded and has just reached the boundaries of the rigid cylinder. At the non-reflecting boundary Γ_∞, the wave front is allowed to pass through the boundary with negligible reflection. At $t = 9$, the wave has begun to reflect off the rigid boundary, creating a complicated backscattered wave.

CONCLUSIONS

In this paper, a space-time finite element method for solution of the transient structural acoustics problem in infinite domains has been presented. The formulation is based on a new multi-field time-discontinuous Galerkin variational equation for both the structure and the acoustic fluid together with their interaction. The resulting algorithm gives an ideal methodology for constructing unstructured finite element meshes in space-time with the optimal combination of good stability and high accuracy.

Desirable attributes of the new approach for computational structural acoustics (CSA) include a natural framework for the design of rigorous *a posteriori* error estimates for self-adaptive solution strategies for unstructured space-time discretizations, and the implementation of high-order accurate and time-dependent non-reflecting boundary conditions. High-order accuracy is obtained simply by raising the order of the space-time polynomial basis functions; both standard nodal interpolation and hierarchical shape functions are accommodated.

New time-dependent non-reflecting boundary conditions written in terms of pressure and velocity variables and which are exact for the first N spherical wave harmonics have been presented. Two new sequences of time-dependent non-reflecting boundary operators were presented; the first involves both time and spatial

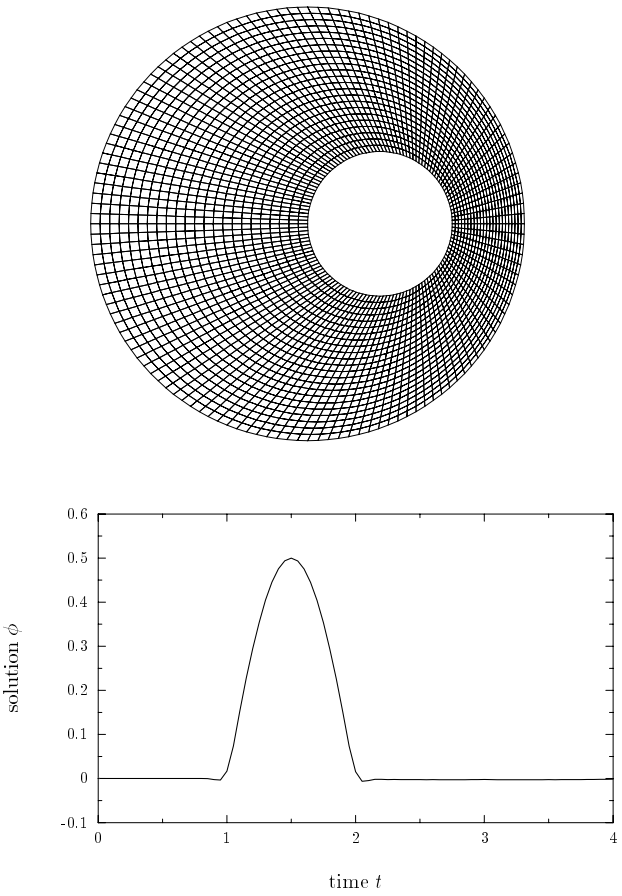

Fig. 4: (Top): Computational domain for a sphere shifted from the centroid of a spherical non-reflecting boundary Γ_∞. Upper half modeled with 1518 axisymmetric elements using quadratic interpolation. (Bottom): Solution time-history on Γ_∞, at the axis of symmetry $\varphi = 0$.

derivatives (local in time and local in space version), and the second involves time derivatives yet retains a spatial integral (local in time and nonlocal in space version). The development of these boundary conditions began with the truncated Dirichlet-to-Neumann (DtN) map in the frequency domain. The time-discontinuous Galerkin space-time formulation provides a natural variational setting for the incorporation of these local in time boundary conditions. Numerical results computed with the space-time formulation demonstrated that with proper usage, the second-order non-reflecting boundary condition $\mathbb{S}_2$, when implemented in the space-time finite element method, is sufficiently accurate to capture the important physics associated with complicated transient radiation and scattering problems involving severe geometric and time scales.

References

[1] W.J. Mansur and C.A. Brebbia. Further developments on the solution of the transient scalar wave equation. In C.A. Brebbia, editor, *Topics in Boundary Element Research*, volume 2, Berlin, 1984. Springer-Verlag.

[2] H.C. Neilson, G.C. Everstine, and Y.F. Wang. Transient response of a submerged fluid-coupled double-walled shell structure to a pressure pulse. *J. Acoust. Soc. Am.*, 70(6):1776–1782, 1981.

[3] A. Safjan, L. Demkowicz, and J.T. Oden. Adaptive finite element methods for hyperbolic systems with application to transient acoustics. *Int. J. Numer. Methods Engng.*, 32:677–707, 1991.

[4] P.M Pinsky and N.N. Abboud. Finite element solution of the transient exterior structural acoustics problem based on the use of radially asymptotic boundary operators. *Comp. Methods in Applied Mech. Engng.*, 85:311–348, 1991.

[5] P.M. Pinsky and L.L. Thompson. Accuracy of local non-reflecting boundary conditions for time-dependent structural acoustics. In *Structural Acoustics*, volume NCA-Vol.12/AMD-Vol.128, pages 153–160. ASME, 1991.

[6] P.M. Pinsky, L.L. Thompson, and N.N. Abboud. Local high order radiation boundary conditions for the two-dimensional time-dependent structural acoustics problem. *J. Acoust. Soc. Am.*, 91(3):1320–1335, 1992.

[7] L.F. Kallivokas and J. Bielak. Time-domain analysis of transient structural acoustics problems based on the finite element method and a novel absorbing boundary element. *J. Acoust. Soc. Am.*, 94(6):3480–3492, 1993.

[8] C. Johnson, U. Navert, and J. Pitkaranta. Finite element methods for linear hyperbolic problems. *Comp. Methods in Applied Mech. Engng.*, 45:285–312, 1984.

[9] C. Johnson. *Numerical Solutions of Partial Differential Equations by the Finite Element Method*. Cambridge University Press, 1986.

[10] T.J.R. Hughes. Recent progress in the development and understanding of SUPG methods with

special reference to the compressible Euler and Navier-Stokes equations. *Int. J. Numer. Methods Engng.*, 7:1261–1275, 1987.

[11] T.J.R. Hughes and G.M. Hulbert. Space-time finite element methods for elastodymamics: Formulations and error estimates. *Comp. Methods in Applied Mech. Engng.*, 66:339–363, 1988.

[12] G.M. Hulbert and T.J.R. Hughes. Space-time finite element methods for second-order hyperbolic equations. *Comp. Methods in Applied Mech. Engng.*, 84:327–348, 1990.

[13] F. Shakib, T.J.R. Hughes, and Z. Johan. A new finite element formulation for computational fluid dynamics: X. the compressible Euler and Navier-Stokes equations. *Comp. Methods in Applied Mech. Engng.*, 89:141–219, 1991.

[14] G. Hauke and T.J.R. Hughes. A unified approach to compressible and incompressible flows. *Comp. Methods in Applied Mech. Engng.*, 113:389–395, 1994.

[15] T.J.R. Hughes, L.P. Franca, and G.M. Hulbert. A new finite element formulation for computational fluid dynamics: VIII. the Galerkin/least-squares method for advective-diffusive equations. *Comp. Methods in Applied Mech. Engng.*, 73:173–189, 1989.

[16] K. Jansen, Z. Johan, and T.J.R. Hughes. Implementation of a one-equation turbulence model within a stabilized finite element formulation of a symmetric advective-diffusive system. *Comp. Methods in Applied Mech. Engng.*, 105:405–433, 1993.

[17] L.L. Thompson. *Design and Analysis of Space-time and Galerkin Least-Squares Finite Element Methods for Fluid-Structure Interaction in Exterior Domains*. PhD thesis, Stanford University, April 1994.

[18] L.L. Thompson and P.M. Pinsky. New space-time finite element methods for fluid-structure interaction in exterior domains. In *Computational Methods for Fluid/Structure Interaction*, volume AMD-Vol. 178, pages 101–120. ASME, 1994.

[19] L.L. Thompson and P.M. Pinsky. A space-time finite element method for structural acoustics in infinite domains, Part I: Formulation, stability, and convergence. *Comp. Methods in Applied Mech. Engng.*, 132:195–227, 1996.

[20] L.L. Thompson and P.M. Pinsky. A space-time finite element method for structural acoustics in infinite domains, Part II: Exact time-dependent non-reflecting boundary conditions. *Comp. Methods in Applied Mech. Engng.*, 132:229–258, 1996.

[21] L.L. Thompson and P.M. Pinsky. A space-time finite element method for the exterior structural acoustics problem: Time-dependent radiation boundary conditions in two spatial dimensions. *Int. J. Numer. Methods Engng.*, 39:1635–1657, 1996.

[22] L.L. Thompson and P.M. Pinsky. A space-time finite element method for the exterior acoustics problem. *J. Acoust. Soc. Am.*, 99(6):3297–3311, 1996.

[23] C. Johnson. Discontinuous Galerkin finite element methods for second order hyperbolic problems. *Comp. Methods in Applied Mech. Engng.*, 107:117–129, 1993.

[24] J.B. Keller and D. Givoli. Exact non-reflecting boundary conditions. *J. Comput. Phys.*, 82(1):172–192, 1989.

[25] M.C. Junger and D. Feit. *Sound, Structures and their Interaction*. M.I.T. Press, Cambridge, MA, 1986.

[26] D. Givoli and J.B. Keller. Non-reflecting boundary conditions for elastic waves. *Wave Motion*, 12:261–279, 1990.

[27] I. Harari. *Computational Methods for Problems of Acoustics with Particular Reference to Exterior Domains*. PhD thesis, Stanford University, 1991.

[28] I. Harari and T.J.R. Hughes. Galerkin/least-squares finite element methods for the reduced wave equation with non-reflecting boundary conditions in unbounded domains. *Comp. Methods in Applied Mech. Engng.*, 98:411–454, 1992.

[29] L.L. Thompson and P.M. Pinsky. A multi-dimensional Galerkin Least-Squares finite element method for time-harmonic wave propagation. In et. al. R. Kleinman, editor, *Second International Conference on Mathematical and Numerical Aspects of Wave Propagation*, pages 444–451. SIAM, 1993.

[30] L.L. Thompson and P.M. Pinsky. A Galerkin Least Squares finite element method for the two-dimensional Helmholtz equation. *Int. J. Numer. Methods Engng.*, 38:371–397, 1995.

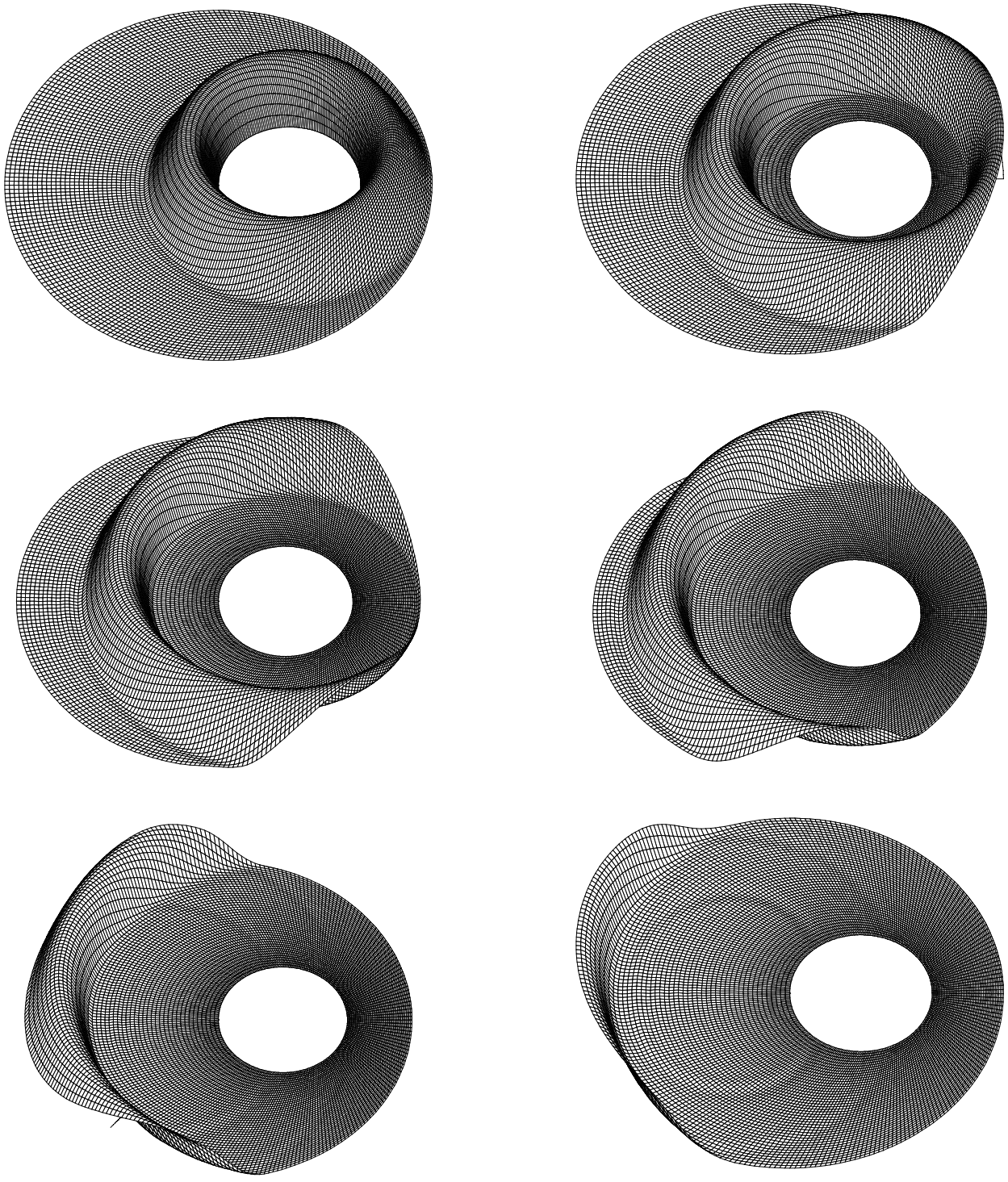

Fig. 5: Radiation from a nonconcentric sphere using the local $\mathbb{S}_2$ absorbing boundary condition: Elevated solution contour for $\phi^h(\boldsymbol{x}\,,\,t)$ shown at the end of the initial pulse $\sin\omega t$ at $t = 1$ and later times $t = 1.5$ through $t = 3.5$ in increments of $\Delta t = 0.5$.

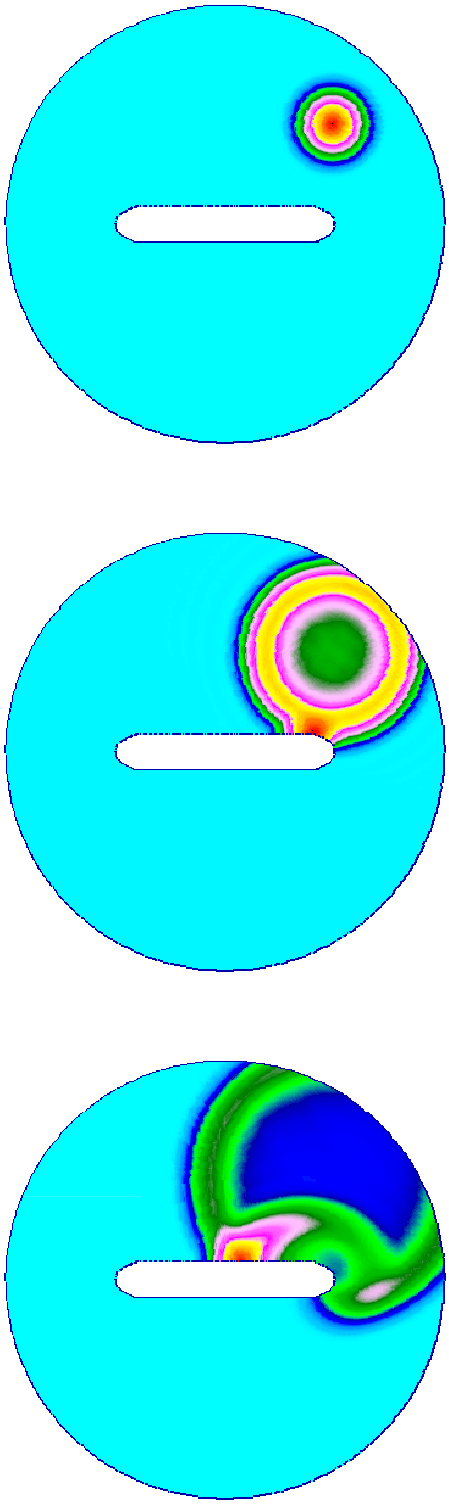

Fig. 6: Scattering from a geometrically complex rigid cylinder due to a point source. Solution contours shown at the end of the initial pulse at $t = 3$ and later times $t = 6$ and $t = 9$.

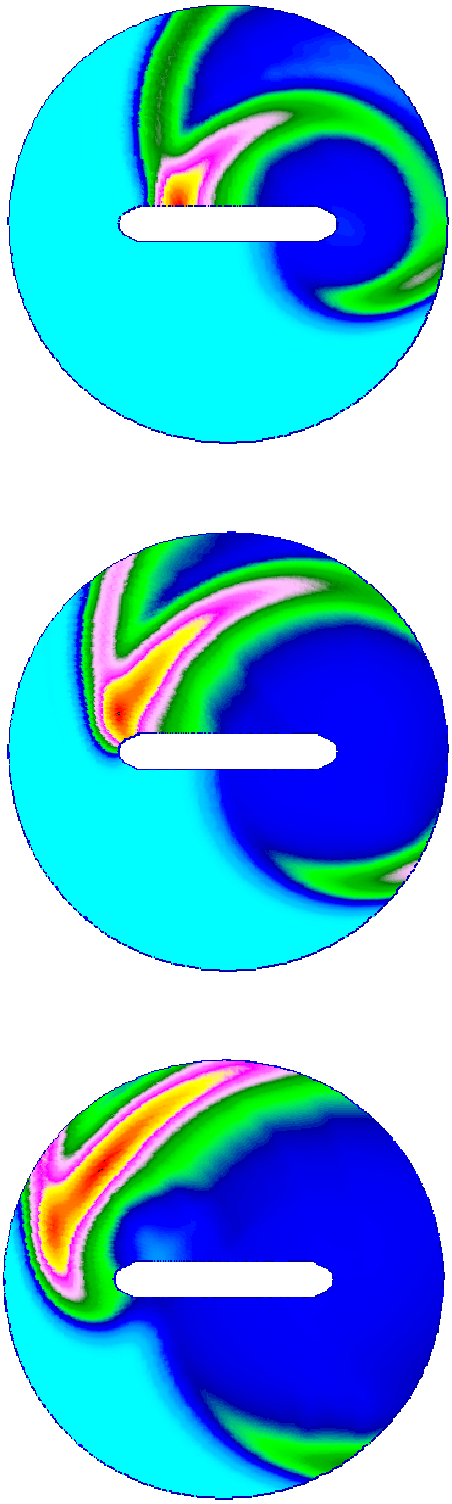

Fig. 7: Scattering from a rigid cylinder due to a point source. Solution contours shown at times $t = 12, 15, 18$.